Optimal tradeoff between exposed and hidden nodes in large wireless networks

ABSTRACT

Wireless networks equipped with the CSMA protocol are subject to collisions due to interference. For a given interference range we investigate the tradeoff between collisions (hidden nodes) and unused capacity (exposed nodes). We determine the optimal sensing range that maximizes throughput and critically depends on the activation rate of nodes. For infinite line networks, we prove the existence of a threshold: When the activation rate is below this threshold the optimal sensing range is small (to maximize spatial reuse). When the activation rate is above the threshold the optimal sensing range is just large enough to preclude all collisions. Simulations suggest that this threshold policy extends to more complex linear and non-linear topologies.

Categories and Subject Descriptors

G.3 [**Probability and Statistics**]: Queueing theory; C.2.1 [**Computer-communication networks**]: Network architecture and design—*wireless communication*

General Terms

Performance, Theory

Keywords

Carrier-sensing range, exposed nodes, hidden nodes, Markov processes, multi-access, throughput, wireless networks

1. INTRODUCTION

Carrier sense multiple-access (CSMA) type protocols form a popular class of medium access protocols for wireless networks. The first CSMA protocol was introduced by Kleinrock and Tobagi [10] in 1975, and has seen many incarnations since, including the widely used 802.11 standard. In this paper we provide an asymptotic analysis of large wireless networks operating under CSMA, in the presence of collisions.

CSMA is a randomized protocol that allows individual nodes to access the medium in a distributed manner. The absence of a centralized scheduler creates more flexibility and allows for the deployment of larger networks. An early example of such a randomized procedure is the ALOHA protocol [1], which forces nodes to wait for some random backoff period before starting a transmission, in order to reduce the likelihood of nearby nodes transmitting simultaneously. The latter event would cause the signals to interfere with each other, and may result in a collision that renders the transmissions useless. CSMA improves upon ALOHA by letting nodes *sense* their surroundings to detect the presence of other transmitting nodes. If a node detects at least one active (i.e. transmitting) node within its sensing range, its backoff timer is frozen, deferring the countdown until the channel is sensed clear. Using this mechanism, collisions can be further reduced.

A key performance measure in wireless networks is throughput, which we define as the average number of successful transmissions per unit of time. Our goal is to investigate the relation between the sensing range and the throughput. The effect of the sensing range can be understood as follows. A small sensing range allows for more simultaneous transmissions, but is less effective in reducing collisions. On the other hand, a large sensing range admits less transmissions, but also mitigates interference. The main contribution of this paper is the examination of this tradeoff in relation to its effect on the throughput.

The network is fully characterized by the sensing range and the interference range. A node can only initiate a new transmission when all nodes within its sensing range are inactive, and this transmission is successful when all nodes within the interference range of the destination node are inactive, and fails otherwise. The network performance suffers from two complementary issues: hidden nodes and exposed nodes (see [15]). Hidden nodes are nodes located outside of the sensing range and therefore not detected by the carrier-sensing mechanism, that may cause collisions at the receivers end. Exposed nodes are nodes that are unnecessarily silenced by CSMA, as they would not interfere with the transmission that triggered the carrier-sensing mechanism. As the sensing range grows, the number of hidden nodes decreases, and the number of exposed nodes increases. In recent years the carrier-sensing tradeoff between hidden and exposed nodes has received much attention [11, 12, 18, 20]. Most of these analytic studies make the assumption that the activity of nodes and their backoff processes are independent, which greatly simplifies the analysis. The interaction between nodes, however, should be taken into account, as it is characteristic for the distributed control and has a large impact on the performance of the network. We do take into account this interaction, by keeping track of the activity of nodes over time. The classical model for such interaction in wireless networks is the one developed in Boorstyn and Kershenbaum [4]. This model has been used in recent years to study throughput-optimality [14] and fairness [7, 8, 17, 16] in a setting without collisions. The stability region for large wireless networks with collisions was investigated in [5].

In the spirit of [4], we model the network as a continuous-time Markov process with interaction between the nodes, so that nodes within a certain distance of an active node are silenced, just as in CSMA. Such interaction is referred to in statistical physics as *hard-core* interaction. This paper is part of a larger program to study wireless networks via hard-core models from statistical physics. Typical for such models is the existence of a Gibbs measure that describes the stationary distribution. This Gibbs measure is normalized by the partition function, which involves a computationally cumbersome summation over all possible configurations. A substantial ingredient of this paper is to characterize and approximate the partition function. We shall consider the network, and thus the partition function, in the asymptotic regime where the number of nodes in the network tends to infinity. For such infinite line networks we are able to obtain structural results on the joint effect of hidden nodes and exposed nodes. We determine analytically the throughput-optimal sensing range that achieves the best tradeoff between reducing hidden nodes and preventing exposed nodes.

The remainder of this paper is structured as follows. In Section 2 we introduce the model, and derive some auxiliary results. Section 3 discusses the main results on the carrier-sensing tradeoff. In Section 4 we perform a detailed study of the partition function. In Section 5 we validate the analytical results for the line network by simulation, and we investigate networks with more general topologies.

2. MODEL DESCRIPTION

We consider a linear array of $2n+1$ nodes, and we denote the set of all nodes by $\mathcal{N} = \{-n, \ldots, n\}$. Whenever a node activates, it transmits a single packet to a neighboring node. With probability γ, the packet is intended for its right neighbor, and with probability $1-\gamma$ for its left neighbor. To accommodate this, we introduce (pure destination) nodes $n+1$ and $-(n+1)$, which receive packets, but do not transmit any packets themselves. We assume all nodes to have the same sensing range β, so that node v has its backoff timer frozen as long as at least one node w for which $|v-w| \leq \beta$ is active (i.e. transmitting), in which case we say that node v is *blocked* by node w.

We assume that all nodes are saturated, meaning that they have an infinite supply of packets available. The duration of the backoff period is assumed to be exponentially distributed with mean $1/\sigma$. Transmissions last for an exponentially distributed duration with unit mean. Under these assumptions, the $(2n+1)$-dimensional process that describes the activity of nodes is a continuous-time Markov process. Each state of the Markov process is described by

$$\omega = (\omega_{-n}, \ldots, \omega_n) \in \{0,1\}^{2n+1}, \tag{1}$$

where $\omega_v = 1$ when node v is active, and $\omega_v = 0$ otherwise. Let $\Omega \subseteq \{0,1\}^{2n+1}$ be the set of all feasible states. Here we call ω *feasible* if no two 1's in ω are β positions or less apart, i.e., $\omega_v \omega_w = 0$ if $1 \leq |v-w| \leq \beta$. Let e_v denote the vector with all zeros, except for a 1 at position v. The Markov process that describes the activity of nodes is then fully specified by the state space Ω and the transition rates

$$r(\omega, \omega') = \begin{cases} \sigma & \text{if } \omega' = \omega + e_v, \\ 1 & \text{if } \omega' = \omega - e_v, \\ 0 & \text{otherwise.} \end{cases} \tag{2}$$

It is well known that this is a reversible Markov process (see [4, 13]) with limiting distribution

$$\pi(\omega) = \begin{cases} Z_{2n+1}^{-1} \prod_{v=1}^{2n+1} \sigma^{\omega_v} & \text{if } \omega \text{ is feasible,} \\ 0 & \text{otherwise,} \end{cases} \tag{3}$$

with Z_{2n+1} the partition function or normalization constant of the probability distribution π. The partition function can be defined recursively as (see [4, 13])

$$Z_i = \begin{cases} 1 + i\sigma & i = 0, 1, \ldots, \beta+1, \\ Z_{i-1} + \sigma Z_{i-\beta-1} & i \geq \beta+2. \end{cases} \tag{4}$$

The sequence $(Z_i)_{i=0}^{\infty}$ is well studied. In fact, for a network with i nodes, Z_i represents the partition function, defined as the summation of probability over all possible states. Straightforward calculations show that the the generating function $G_Z(x)$ of Z_i can be written as (see e.g. Pinksy and Yemini [13])

$$G_Z(x) = \sum_{i=1}^{\infty} Z_i x^i = \frac{x - 1 + \sigma x^{\beta+1} - \sigma x}{(x-1)(1 - x - \sigma x^{\beta+1})}. \tag{5}$$

Let $\lambda_0, \ldots, \lambda_\beta$ denote the $\beta+1$ roots of

$$\lambda^{\beta+1} - \lambda^{\beta} - \sigma = 0. \tag{6}$$

Applying partial fraction expansion to (5) yields the following result (proved in Section 6):

PROPOSITION 1. *The partition function Z_i is given by*

$$Z_i = \sum_{j=0}^{\beta} c_j \lambda_j^i \quad , i = 0, 1, \ldots, \tag{7}$$

where λ_j are the roots of (6)*, and*

$$c_j = \frac{\lambda_j^{\beta+1}}{(\beta+1)\lambda_j - \beta}. \tag{8}$$

To model interference, we introduce an interference range η. A transmission succeeds if and only if at the start of this transmission no nodes within distance η of the receiving node are already active. This type of interference is referred to in the literature as the *perfect capture* collision model [4]. Note that neither (2) nor (3) depends on η, as collisions have no impact on the dynamics of the system. Using the sensing range β and interference range η we can define formally hidden nodes and exposed nodes. Denote by $\mathcal{H}_r$ ($\mathcal{H}_l$) the set of hidden nodes due to transmissions from node 0 to node 1 (node -1): all nodes outside the sensing range of

0, but within the interference range of the receiving node 1. By $\mathcal{E}_r$ ($\mathcal{E}_l$) we denote the set of nodes to which this transmission is exposed, so all nodes within the sensing range of 0, but outside the interference range of the receiving node. For completeness we let $\mathcal{B}_r$ ($\mathcal{B}_l$) denote the set of all remaining nodes that block transmissions from node 0 to 1 (-1). This yields:

$$\begin{aligned}
\mathcal{H}_r &= \{v \in \mathcal{N} \mid |v| \geq \beta+1,\ |v-1| \leq \eta\},\\
\mathcal{H}_l &= \{v \in \mathcal{N} \mid |v| \geq \beta+1,\ |v+1| \leq \eta\},\\
\mathcal{E}_r &= \{v \in \mathcal{N} \mid |v| \leq \beta,\ |v-1| \geq \eta+1\},\\
\mathcal{E}_l &= \{v \in \mathcal{N} \mid |v| \leq \beta,\ |v+1| \geq \eta+1\},\\
\mathcal{B}_r &= \{v \in \mathcal{N} \mid |v| \leq \beta,\ |v-1| \leq \eta\},\\
\mathcal{B}_l &= \{v \in \mathcal{N} \mid |v| \leq \beta,\ |v+1| \leq \eta\}.
\end{aligned}$$

An example is given in Figure 1(a). Node 3 is a hidden node, as it interferes with the transmission from node 0 to node 1 ($\eta = 2$) despite the carrier-sensing mechanism ($\beta = 1$). In Figure 1(b) node 0 is an exposed node because it would not interfere ($\eta = 2$) with the transmission from node 2 to node 3 and is therefore unnecessarily silenced by the carrier-sensing mechanism ($\beta = 2$).

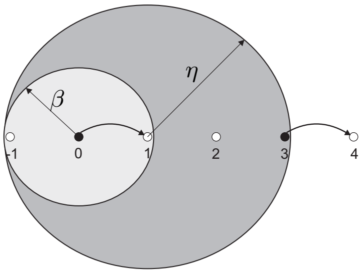

(a) Node 3 is a hidden node, and may interfere with the transmission between nodes 0 and 1.

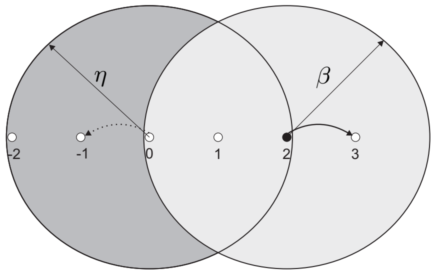

(b) Node 0 is an exposed node, unnecessarily silenced by the transmission between nodes 2 and 3.

Figure 1: Examples of hidden and exposed nodes.

We focus on node 0 (the node in the middle of the network) and in particular its throughput $\theta_n(\beta, \eta, \sigma)$ defined as the average number of successful transmissions per unit of time.

PROPOSITION 2. *The throughput of node 0 is given by*

$$\theta_n(\beta, \eta, \sigma) = \sigma \frac{Z_{n-\max\{\beta,\eta-1\}} Z_{n-\max\{\beta,\eta+1\}}}{Z_{2n+1}}. \tag{9}$$

PROOF. Denote by θ_r (θ_l) the rate of successful transmission of node 0 to node 1 (node -1), so $\theta_n(\beta, \eta, \sigma) = \theta_r + \theta_l$. The activation attempts to node 1 (node -1) occur according to a Poisson process with rate $\sigma\gamma$ ($\sigma(1-\gamma)$). We first consider activation attempts to node 1. Whether or not an activation attempt is successful depends on the state of the system. Define

$$\begin{aligned}
A_1 &= \{\omega \in \Omega \mid \exists v \in \mathcal{B}_r \cup \mathcal{E}_r : \omega_v = 1\},\\
A_2 &= \{\omega \in \Omega \mid \forall v \in \mathcal{B}_r \cup \mathcal{E}_r : \omega_v = 0,\ \exists v \in \mathcal{H}_r : \omega_v = 1\},\\
A_3 &= \{\omega \in \Omega \mid \forall v \in \mathcal{B}_r \cup \mathcal{E}_r \cup \mathcal{H}_r : \omega_v = 0\}.
\end{aligned}$$

When the system is in state $\omega \in A_1$, the attempt is blocked and node 0 remains in its current state. When the system is in a state $\omega \in A_2$, node 0 is not blocked so it activates. However, at least one hidden node is active so the transmission fails does not contribute to the throughput. When the system in in state $\omega \in A_3$, the perfect capture assumption guarantees a successful transmission. It follows from the PASTA property (cf. [2]) that the probability of an arbitrary activation attempt resulting in a successful transmission is equal to the limiting probability of the system being in a state $\omega \in A_3$, $\sum_{\omega \in A_3} \pi(\omega)$. So the rate of successful transmissions initialized (and thus the throughput) is given by

$$\theta_r = \sigma\gamma \sum_{\omega \in A_3} \pi(\omega). \tag{10}$$

From the definitions of $\mathcal{B}_r$, $\mathcal{E}_r$ and $\mathcal{H}_r$ we see that

$$A_3 = \{\omega \in \Omega \mid \forall v \in (D_1 \cup D_2)^c : \omega_v = 0\}, \tag{11}$$

where

$$\begin{aligned}
D_1 &= \{-n, \ldots, -\max\{\beta, \eta-1\} - 1\},\\
D_2 &= \{\max\{\beta, \eta+1\} + 1, \ldots, n\}.
\end{aligned} \tag{12}$$

Let Z_D denote the partition function for a subset of nodes $D \subseteq \mathcal{N}$. Then

$$\theta_r = \sigma\gamma \frac{Z_{D_1 \cup D_2}}{Z_{\mathcal{N}}}. \tag{13}$$

The model on the line has the property that by conditioning on the activity of one of the nodes, its state space can be decomposed, leading to two smaller instances of the same model on the line. In particular, we know that $Z_{D_1 \cup D_2} = Z_{D_1} Z_{D_2}$ (see [4, Equation (15)]), so that

$$\begin{aligned}
\theta_r &= \sigma\gamma \frac{Z_{D_1} Z_{D_2}}{Z_{\mathcal{N}}}\\
&= \sigma\gamma \frac{Z_{n-\max\{\beta,\eta-1\}} Z_{n-\max\{\beta,\eta+1\}}}{Z_{2n+1}},
\end{aligned} \tag{14}$$

where $Z_i := Z_{\{-n,-n+i-1\}}$ denotes the partition function of a network with i consecutive nodes on a line. Similarly,

$$\theta_l = \sigma(1-\gamma) \frac{Z_{n-\max\{\beta,\eta-1\}} Z_{n-\max\{\beta,\eta+1\}}}{Z_{2n+1}}. \tag{15}$$

and (9) follows. □

3. MAIN RESULTS

Our principal aim is to choose the sensing range β so that throughput $\theta_n(\beta, \eta, \sigma)$ is maximized. Define

$$\beta_n^* = \underset{\beta}{\operatorname{argmax}}\, \theta_n(\beta, \eta, \sigma). \tag{16}$$

Determining β_n^* corresponds to quantifying and optimizing the tradeoff between preventing collisions through interference (preventing hidden nodes by setting β large) and allowing harmless transmissions (preventing exposed nodes by setting β small). We want to obtain structural insights in how to choose β_n^*, and for this purpose the expressions for Z_i in (7) and $\theta_n(\beta, \eta, \sigma)$ in (9) are too cumbersome. Therefore, we investigate the throughput in the regime where the network becomes large ($n \to \infty$), so that (9) simplifies considerably, allowing for more explicit analysis. The analytic results that we obtain for the infinite network provide remarkably sharp approximations for the finite network; see Section 5.1. All proofs that are not given in this section are provided in Section 6.

We start by presenting the limiting expression for $\theta_n(\beta, \eta, \sigma)$ as the size of network becomes infinite:

Proposition 3. *Let* λ_0 *denote the unique positive real root of* (6). *Then*

$$\theta(\beta, \eta, \sigma) = \lim_{n\to\infty} \theta_n(\beta, \eta, \sigma) = \sigma \frac{\lambda_0^{\beta - f(\beta)}}{(\beta+1)\lambda_0 - \beta}, \tag{17}$$

where

$$f(\beta) = \begin{cases} 2\eta & \text{if } 0 \leq \beta \leq \eta - 1, \\ \eta + \beta + 1 & \text{if } \eta - 1 \leq \beta \leq \eta + 1, \\ 2\beta & \text{if } \beta \geq \eta + 1. \end{cases} \tag{18}$$

Proof. From Rouché's theorem (see De Bruijn [6]) it readily follows that $\lambda_0 > |\lambda_j|$ for $j = 1, \dots, \beta$, and so from (7) we get

$$Z_i = c_0 \lambda_0^i \left(1 + o(1)\right), \quad i \to \infty, \tag{19}$$

and hence

$$\lim_{n\to\infty} \theta_n(\beta, \eta, \sigma) = \lim_{n\to\infty} \sigma \frac{c_0 \lambda_0^{n-\max\{\beta,\eta-1\}} c_0 \lambda_0^{n-\max\{\beta,\eta+1\}}}{c_0 \lambda_0^{2n+1}}$$
$$= \sigma c_0 \lambda_0^{-\max\{\beta,\eta-1\}-\max\{\beta,\eta+1\}-1},$$

which yields (18). □

Now that we have the limiting expression for the throughput in (17) we opt for an asymptotic analysis. That is, instead of searching for β_n^*, we shall search for its asymptotic counterpart

$$\beta^* = \operatorname*{argmax}_{\beta} \theta(\beta, \eta, \sigma), \tag{20}$$

where we henceforth consider θ as a continuous function of β. In Section 5.1 we show that the errors $|\theta_n - \theta|$ and $|\beta_n^* - \beta^*|$ become small, already for moderate values of n. Because we consider from here onwards an infinite line of nodes, all nodes have the same number of nodes within their sensing range. This removes all boundary effects, and all nodes have the same throughput, which is why just investigating node 0 is sufficient to investigate the entire network.

Proposition 4. $\beta^* \in [\eta - 1, \eta + 1]$.

The result of Proposition 4 can be understood as follows. By increasing β beyond $\eta + 1$, no additional collisions are prevented, but an increasing number of nodes is silenced. On the other hand, the nodes that become unblocked when decreasing β below $\eta - 1$, cause collisions when activated. Note that for all values $\beta \in [\eta - 1, \eta + 1]$, we can rewrite (17) as

$$\theta(\beta, \eta, \sigma) = g(\beta) \cdot \frac{(\lambda_0(\beta))^{\beta - \eta - 1}}{\beta + 1} \tag{21}$$

with

$$g(\beta) = \frac{\lambda_0(\beta) - 1}{\lambda_0(\beta) - \frac{\beta}{\beta+1}} \to 1, \quad \beta \to \infty. \tag{22}$$

We are now in the position to present our main result. While we already know that the optimal sensing range is contained in the interval $[\eta - 1, \eta + 1]$, we shall be more specific.

Theorem 1. *There exists a threshold interval* $[\sigma_{\min}, \sigma_{\max}]$ *such that*

$$\beta^* = \begin{cases} \eta - 1 & \text{if } \sigma \leq \sigma_{\min}, \\ \eta + 1 & \text{if } \sigma \geq \sigma_{\max}, \end{cases} \tag{23}$$

and $\beta^* \in (\eta - 1, \eta + 1)$ *if* $\sigma \in (\sigma_{\min}, \sigma_{\max})$.

The proof of Theorem 1 follows from a detailed study of $\theta(\beta, \eta, \sigma)$ which involves implicit differentiation with respect to β (since $\lambda_0(\beta)$ is defined implicitly).

Theorem 1 can be interpreted as follows (see Figure 2). When the nodes are aggressive (σ large) nodes activate very quickly after finishing their previous transmissions. In the language of statistical physics, the system temperature decreases, and the system typically gets stuck in maximal independent sets of active nodes (the configurations with the highest energy level). When the system is in a maximal independent set, and if collisions are not ruled out, an activating node suffers a collision almost surely. This explains why for σ large, the optimal sensing range is $\beta = \eta + 1$, preventing collisions completely. On the other hand, when nodes are not aggressive (σ small) collisions become rare, as few nodes are active simultaneously. In this case, throughput is best served by increasing the spatial reuse, that is, decreasing the sensing range. This explains the result of Theorem 1 for σ small.

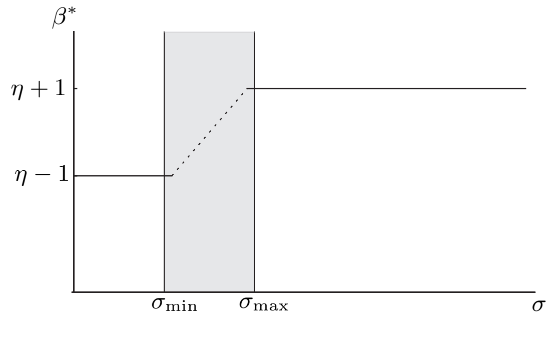

Figure 2: The optimal range β^* plotted as a function of σ.

Note that Theorem 1 does not give the exact value for β^* for $\sigma \in (\sigma_{\min}, \sigma_{\max})$. We shall not pursue this further. Instead, we prove in our next result that the threshold interval $[\sigma_{\min}, \sigma_{\max}]$ is small. Introduce the constant $\tau = (\sqrt{5}-1)/2$.

THEOREM 2. *Let $\kappa = \frac{\tau}{\eta+1}$. The threshold interval is bounded as*

$$[\sigma_{\min}, \sigma_{\max}] \subseteq [\kappa(1+\kappa)^{\eta-1}, \kappa(1+\kappa)^{\eta+1}]. \tag{24}$$

The bounds in (24) for $\sigma_{\min}$ and $\sigma_{\max}$ are sharp; see Section 5.1 for an example.

PROPOSITION 5. *The length of the threshold interval is asymptotically given as*

$$\sigma_{\max} - \sigma_{\min} \sim \frac{2e^{\tau}}{7+4\tau}\left(\frac{1}{\eta+1}\right)^2 \quad \text{as } \eta \to \infty. \tag{25}$$

Here we say that $f(\eta) \sim g(\eta)$ if $f(\eta)/g(\eta) \to 1$ as $\eta \to \infty$. From Proposition 5 we see that the length of the threshold interval is $\mathcal{O}(\eta^{-2})$. Therefore, the interval length decreases rapidly as a function of η, and we can speak of an almost immediate jump from one regime ($\beta^* = \eta - 1$) to the other ($\beta^* = \eta + 1$).

3.1 Throughput limiting behavior

We now consider some limiting regimes for which we can make more explicit statements about the throughput. From Theorem 2 we can already see that the threshold interval moves in the direction of zero as η becomes large, which implies that the $\beta^* = \eta + 1$ already for small values of σ. The next result shows that in the regime where η becomes large, the maximum throughput tends to zero.

PROPOSITION 6. *Let $\sigma > 0$ be fixed. As $\eta \to \infty$,*

$$\max_{\beta} \theta(\beta, \eta, \sigma) = \frac{1}{\eta+2}\left(1 + \mathcal{O}\left(\frac{1}{\ln(\eta+1)}\right)\right). \tag{26}$$

For $\beta \geq \eta+1$ our model reduces to a model without collisions that was studied extensively in [4, 13, 3, 19, 9, 16]. In particular, one immediately obtains from (17) the following result:

COROLLARY 1. *Let $\beta \geq \eta + 1$. Then*

$$\theta(\beta, \eta, \sigma) = \sigma \frac{\lambda_0^{-\beta}}{(\beta+1)\lambda_0 - \beta}. \tag{27}$$

This result was also derived in [13, 3, 19, 9]. On inspection of (27) we see that the throughput is approximately $\frac{1}{\beta+1}$ when either σ or β is large. This can be understood as follows. For large σ, the high activity rate allows for configurations close to the maximal independent: a configuration in which one out of every $\beta + 1$ nodes in active. For β large, when a node deactivates a large number of neighboring nodes become eligible for activation. The time until the first such node activates goes to 0 when β increases.

COROLLARY 2. *Let $\beta \leq \eta$. Then*

$$\lim_{\sigma \to \infty} \theta_n(\beta, \eta, \sigma) = 0. \tag{28}$$

PROOF. From (39) it follows that

$$\lambda_0(\sigma) = \sigma^{\frac{1}{1+\beta}} + \mathcal{O}(1), \quad \sigma \to \infty. \tag{29}$$

Substituting (29) into the throughput (17), and using that $f(\beta) > 2\beta$ when $\beta \leq \eta$, yields

$$\theta_n(\beta, \eta, \sigma) = \frac{\sigma(\sigma^{\frac{1}{1+\beta}} + \mathcal{O}(1))^{\beta - f(\beta)}}{(\beta+1)(\sigma^{\frac{1}{1+\beta}} + \mathcal{O}(1)) - \beta} \to 0, \quad (\sigma \to \infty), \tag{30}$$

which gives (28). □

Figure 3 shows the throughput plotted against the activity rate σ for $\eta = 7$ and various values of β. Clearly, when $\beta \leq \eta$, the throughput gradually drops to 0, whereas for $\beta \geq \eta + 1$, the throughput approaches the limit $1/(\beta + 1)$. This confirms Corollaries 1 and 2.

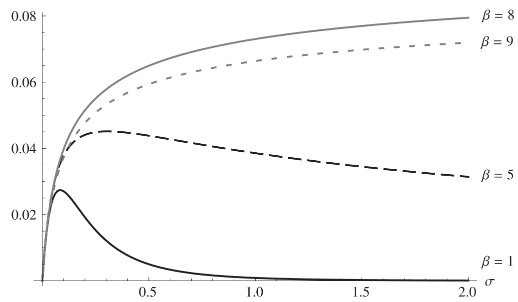

Figure 3: The throughput $\theta(\beta, \eta, \sigma)$ plotted against σ for $\eta = 7$ and various values of β.

4. PARTITION FUNCTION ROOTS

In this section we study the roots $\lambda_0, \ldots, \lambda_\beta$ of (6) in more detail. In particular, we derive exact infinite-series expressions for the roots that are used in this paper both for numerical purposes (in Section 5) and to prove Corollary 2. Our main tool will be Lagrange inversion (see [6]), and depending on the value of σ, this gives two different infinite-series expressions. Let $(x)_n = \Gamma(x+n)/\Gamma(x)$ denote the Pochhammer symbol.

PROPOSITION 7. *For small $\sigma > 0$,*

$$\lambda_0(\sigma) = 1 + \sum_{l=1}^{\infty} \frac{(-1)^{l-1}(\beta l)_{l-1}}{l!}\sigma^l, \tag{31}$$

$$\lambda_j(\sigma) = \sum_{l=1}^{\infty} \frac{(l/\beta)_{l-1}}{l!} w_j^l, \quad j = 1, 2, \ldots, \beta, \tag{32}$$

where $w_j = \sigma^{1/\beta} e^{2\pi\imath(j-1/2)/\beta}$. The series expansions in (31) *and* (32) *converge for*

$$0 \leq \sigma \leq \frac{\beta^\beta}{(\beta+1)^{\beta+1}} =: \xi(\beta), \tag{33}$$

and diverge otherwise.

PROOF. We first consider the case $j = 0$. Set $\mu_0 = \lambda_0 - 1$, so μ_0 satisfies $\mu_0(1+\mu_0)^\beta = \sigma$. Hence for small values of $|\sigma|$ we have

$$\mu_0 = \sum_{l=1}^{\infty} \frac{1}{l!} \left(\frac{\mathrm{d}}{\mathrm{d}\mu}\right)^{l-1} \left[\left(\frac{\mu}{\mu(1+\mu)^\beta}\right)^l\right]_{\mu=0} \sigma^l$$
$$= \sum_{l=1}^{\infty} \frac{(-1)^{l-1}(\beta l)_{l-1}}{l!} \sigma^l. \quad (34)$$

Next we consider the case that $j = 1, \ldots, \beta$. We now write (6) as

$$\lambda^\beta(1-\lambda) = -\sigma, \quad \lambda(1-\lambda)^{1/\beta} = w_j, \quad (35)$$

where

$$w_j = \sigma^{1/\beta} \mathrm{e}^{2\pi\imath(j-1/2)/\beta}. \quad (36)$$

Now we get for $|w_j|$ sufficiently small

$$\lambda_j = \sum_{l=1}^{\infty} \frac{1}{l!} \left(\frac{\mathrm{d}}{\mathrm{d}\lambda}\right)^{l-1} \left[\left(\frac{\lambda}{\lambda(1-\lambda)^{1/\beta}}\right)^l\right]_{\lambda=0} w_j^l$$
$$= \sum_{l=1}^{\infty} \frac{(l/\beta)_{l-1}}{l!} w_j^l. \quad (37)$$

The radii of convergence of the series in (34) and (37) are easily obtained from the asymptotics

$$\Gamma(x+1) = x^{x+1/2}\mathrm{e}^{-x}\sqrt{2\pi}(1+\mathcal{O}(x^{-1}), \quad x \to \infty, \quad (38)$$

of the Γ-function, used to examine the Pochhammer quantities $(x)_n = \Gamma(x+n)/\Gamma(x)$ and the factorials $l! = \Gamma(l+1)$ that occur in both series. This yields the result that both series converge when $|\sigma| \le \xi(\beta)$ and diverge for $|\sigma| > \xi(\beta)$. When $|\sigma| = \xi(\beta)$ the terms in either series are $\mathcal{O}(l^{-3/2})$. □

PROPOSITION 8. *For large $\sigma > 0$,*

$$\lambda_j(\sigma)^{-1} = \sum_{l=1}^{\infty} \frac{\left(\frac{-l}{\beta+1}\right)_{l-1}}{l!} v_j^{-l}, \quad (39)$$

where $v_j = \sigma^{1/(\beta+1)}\mathrm{e}^{2\pi\imath j/(\beta+1)}$. The series expansion in (39) *converges for*

$$\sigma \ge \xi(\beta), \quad (40)$$

and diverges otherwise.

PROOF. We can treat the cases $j = 0$ and $j = 1, \ldots, \beta$ simultaneously now. We write (6) in the form

$$\frac{1}{\lambda}\left(1 - \frac{1}{\lambda}\right)^{\frac{-1}{\beta+1}} = \left(\frac{1}{\sigma}\right)^{\frac{1}{\beta+1}} = v^{-1}, \quad (41)$$

where we let

$$v^{-1} = v_j^{-1} = \left(\frac{1}{\sigma}\right)^{\frac{1}{\beta+1}} \mathrm{e}^{-2\pi\imath\frac{j}{\beta+1}}, \quad j = 0, 1, \ldots, \beta \quad (42)$$

with $\sigma^{-\frac{1}{\beta+1}} > 0$ in (42). We get for sufficiently large σ that (letting $u = 1/\lambda$)

$$\frac{1}{\lambda_j} = \sum_{l=1}^{\infty} \frac{1}{l!} \left(\frac{\mathrm{d}}{\mathrm{d}u}\right)^{l-1} \left[\left(\frac{u}{u(1-u)^{-1/(\beta+1)}}\right)^l\right]_{u=0} v_j^{-l}$$
$$= \sum_{l=1}^{\infty} \left(\frac{-l}{\beta+1}\right)_{l-1} \frac{v_j^{-l}}{l!}. \quad (43)$$

The Pochhammer quantity $(\frac{-l}{\beta+1})_{l-1}$ vanishes if and only if $l = 1, 2, \ldots$ is a multiple of $\beta+1$. The radius of convergence of the series in (43) is again determined by the asymptotics of the Γ-function in (38). Here it must also be used that

$$\Gamma(-J) = \frac{-1}{\Gamma(J+1)} \frac{\pi}{\sin \pi J}, \quad J > 0. \quad (44)$$

It follows that the series in (43) is convergent when $|\sigma| \ge \xi(\beta)$ and divergent when $|\sigma| < \xi(\beta)$. When $|\sigma| = \xi(\beta)$ the terms in the series are $\mathcal{O}(l^{-3/2})$. □

Figure 4 shows the roots of (6) drawn in the complex λ-plane for $\beta = 4$. Each line corresponds to a root as a function of σ, and the dots represent the threshold $|\sigma| = \xi(\beta)$. The dashed curved encircling the origin 0 and the point 1 is the image of $v \in \mathbb{C}$ with $|v| = \sigma^{1/(\beta+1)}$ under the mapping given by the inverse of the right-hand side of (39) with v_j replaced by v.

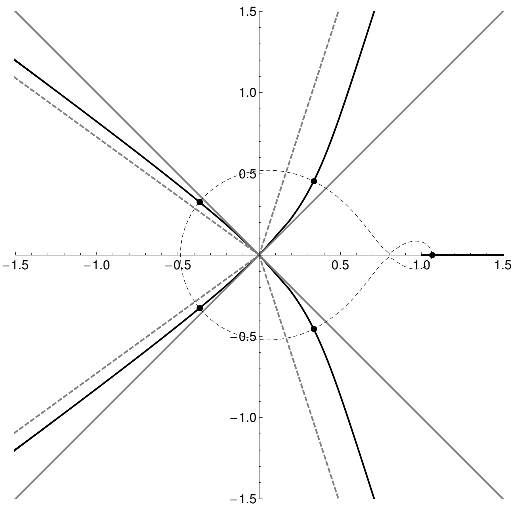

Figure 4: The roots of $\lambda^{\beta+1} + \lambda^\beta = \sigma$ as functions of σ in (31), (32) and (39), for $\beta = 4$.

5. DISCUSSION AND OUTLOOK

The distinguishing feature of this paper is the presence of node interaction when making the tradeoff between hidden nodes and exposed nodes. In order to get a handle on the throughput function (and hence the partition function) we studied the wireless network in the asymptotic regime on the infinitely many nodes. This resulted in a tractable limiting expression for the throughput of node zero (and hence any other node) that allowed us to prove the following two results:

(i) To optimize the throughput, one should always choose a sensing range β that is close to the interference range η, and in fact the optimal sensing range is contained in the interval $[\eta-1,\eta+1]$ (see Proposition 4).

(ii) The sensing range β^* that optimizes the throughput equals $\eta-1$ for less aggressive systems (small σ) and $\eta+1$ for aggressive systems (large σ). In fact, we were able to show the existence of a threshold interval for σ that distinguishes these two regimes (Theorem 1). This important result provides (partial) justification for the frequently made assumption that no collisions occur. Indeed, one key take away is that if σ is large enough, ruling out all collisions by setting $\beta=\eta+1$ is optimal.

We have further shown that the threshold interval is in many cases small, which implies that one can speak of an almost immediate jump from one regime ($\beta^*=\eta-1$) to the other ($\beta^*=\eta+1$). We have argued that indeed, when the aggressiveness of the system is large enough, say σ larger than some value σ^*, the system no longer gains from the potential benefits of more flexibility (small β), and just settles for the situation with no collisions.

We shall now discuss two remaining issues. In Section 5.1 we investigate to what extent the asymptotic results give accurate predictions for finite line networks. In Section 5.2 we investigate whether the notions of two regimes and a critical threshold carry over to more general topologies.

5.1 Finite versus infinite line networks

We shall now look at the approximation error $|\theta_n-\theta|$ and the resulting error in the optimal sensing range. To investigate the error we plot θ_n and θ in Figure 5, represented by the dashed line and the solid line, respectively. All results for θ_n were obtained by using (9) in combination with the infinite-series expressions for the roots in Section 4.

We take $n=100$ (i.e., 201 nodes), $\eta=4$, and we let β increase from 1 to 100. In Figure 5(a) $\sigma=0.25$, and in Figure 5(b) $\sigma=5$. For β small the error $|\theta_n(\beta)-\theta(\beta)|$ is negligible, but the error increases as β increases. This can be explained by the observation that for larger β, the number of roots of (6) increases, as does the number of roots discarded by the approximation. This phenomenon becomes more pronounced for larger values of σ. The non-monotone behavior of θ_n is caused by the fact that for finite n, the system is directed to maximal independent sets of active nodes, in particular for σ large, and these sets change dramatically with β. The most important observation is that the error $|\theta_n-\theta|$ is small for those values of β that lead to a large throughput. Figure 6 is similar to Figure 5, but instead of fixing n and varying β, we set $\beta=16$ and vary n. In Figure 6(a) we take $\sigma=0.2$ and in Figure 6(b) we take $\sigma=5$. The quality of the approximation increases with n.

Figure 7 shows the optimal sensing range plotted against σ, for $\eta=5$. Each of the Figures 7(a)-7(d) shows the optimal range $\beta_n^*(\sigma)$ for finite n. We take $\eta=5$ for all figures, and let σ increase from 0.15 to 0.19. The vertical lines indicate the bounds on the threshold interval from Theorem 2, and we see that these bounds are sharp. The optimal sensing range β^* for $n\to\infty$ behaves as predicted by Theorem 1, jumping from $\eta-1$ before the threshold interval, to $\eta+1$ after this interval, and β_n^* shows a similar pattern. We conclude that

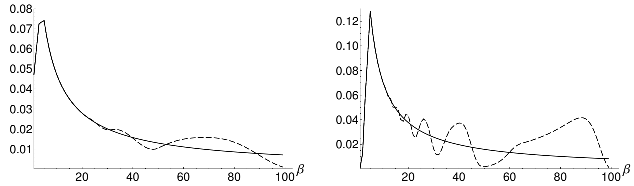

(a) $\sigma=0.25$. (b) $\sigma=5$.

Figure 5: The throughput θ_n (dashed) and θ (solid) plotted against β (with $n=100$).

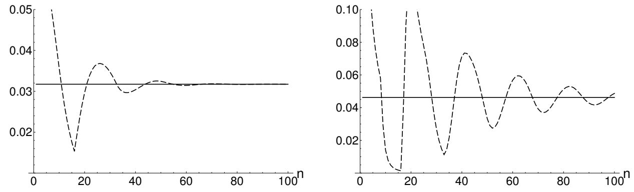

(a) $\sigma=0.2$. (b) $\sigma=5$.

Figure 6: The throughput θ_n (dashed) and θ (solid), plotted against n (with $\beta=16$).

$n=\infty$ provides a good approximation for the behavior of finite-sized networks, already for small and moderate values of n

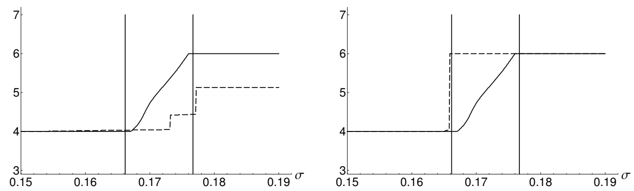

(a) $n=15$. (b) $n=20$.

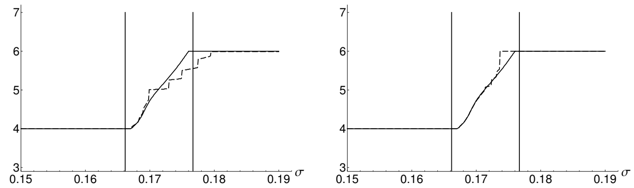

(c) $n=25$. (d) $n=30$.

Figure 7: The optimal sensing range β_n^* (dashed) and β^* (solid) plotted against σ around the threshold interval for various values of n.

5.2 General topologies

To investigate more general topologies, we first need a more elaborate description of the model. In addition to nodes, we introduce directed links between nodes that represent the possibility of transmissions taking place between these nodes. For two nodes to be able to transmit data, we require them to be within (Euclidian) distance m of each other. We assume links are formed between all nodes within distance m. Each node has activation rate σ, and the destination of a transmission is chosen uniformly from all links originating from the activating node. The blocking range and interference range are also defined according to the Euclidian distance.

First we consider 16 nodes placed on a 4×4 grid at unit distance from each other. The grid is wrapped around (the top is connected to the bottom, and the left side to the right side) so the network is fully symmetric and all nodes have the same environment (and the same throughput), eliminating boundary effects. We set $m = 1$ and construct links between neighboring nodes (see Figure 8(a)). We take $\eta = 1$ and $\beta = 0, 1, 1.5, 2$.

Figure 8(b) shows the average per-node throughput plotted against σ. For σ small we see that $\beta = 0$ (i.e. $\beta = \eta - m$) is throughput-optimal, and for σ large it turns out $\beta = 2$ ($\beta = \eta + m$) is optimal. Moreover, when β is such that it allows collisions ($\beta < 2$), we see that the throughput decreases when σ increases, while for $\beta = 2$ the throughput approaches a non-zero limiting value for large σ.

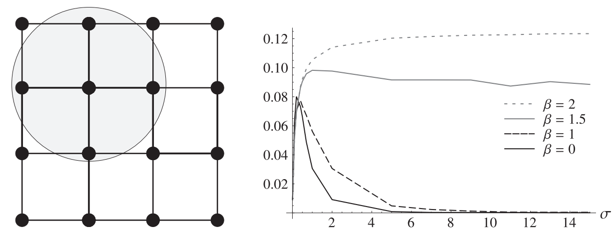

(a) 16 nodes on a 4×4 grid.

(b) The throughput θ of an arbitrary node in a grid, plotted against σ.

Figure 8: A grid network and the corresponding per-node throughput.

We next show in Figure 9 a randomly generated network with 16 nodes. The transmission ranges are indicated by the circles, and links are displayed as lines. We assume a transmission range of $m = 1$ and interference range $\eta = 1.6$. Links are formed between all nodes within distance m and when a node activates it uniformly chooses a node within distance m as the receiver.

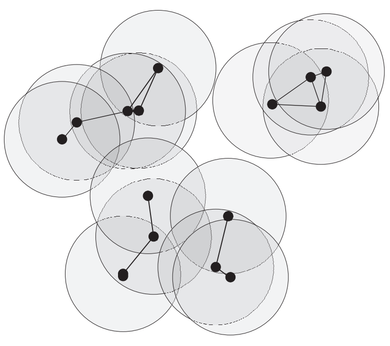

Figure 9: Random network with 16 nodes.

The simulation results are shown in Figure 10. The average per-node throughput is plotted against σ for $\beta = 0.2, 0.3, 1, 1.3, 1.5$. Figure 10 shows resemblance with Figure 3 for the infinite line. For β small the throughput drops as σ increases, as collisions let deteriorate the throughput. For large β collisions are precluded, and the average throughput stabilizes. Moreover, we see that the optimal sensing range β^* again depends on σ. For $\sigma < 0.1$ we have $\beta^* = 0.3$ (this is not visible in the picture), whereas for $\sigma > 0.1$ the optimal sensing range is $\beta^* = 1$.

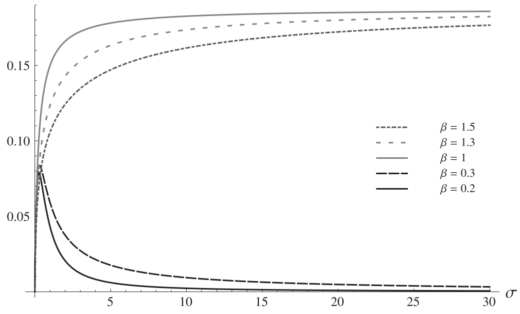

Figure 10: The average per-node throughput plotted against σ.

The tradeoff for individual nodes in an irregular network is more complicated. Although we see a similar threshold interval $(\sigma_{\min}, \sigma_{\max})$ that separates two sensing regimes, the position of the threshold interval and the optimal sensing ranges may differ between nodes. This depends on the direct surroundings of the node, as well as on the entire network structure.

5.3 Future work

Wireless networks equipped with CSMA on complex topologies form highly relevant objects for further study. In particular, we have raised the question whether a threshold interval for the activity rate σ exists, which says that the optimal sensing ranges equals β_L for σ below the interval, and β_U for σ above the interval. For the two examples in Section 5.2 there is indeed such a threshold interval, but a more thorough study is needed.

Obtaining numerical results for complex topologies with many nodes is challenging. For one thing, the state space no longer decomposes (as with the line network), so that the calculation of the partition function becomes more involved. In determining the stationary distribution, and hence the throughput of nodes, the brute-force method would be to sum over all possible configurations, but that will become computationally cumbersome, already for moderate instances of the network. Alternative approaches would be to use limit theorems, for instance for highly dense networks with many nodes. We conjecture that in such networks we would again find a threshold interval that distinguishes two regimes for the optimal sensing range.

6. REMAINING PROOFS

6.1 Proof of Proposition 1

We write the generating function from (5) as

$$Z(x, \sigma) = \frac{P(x)}{S(x)}, \tag{45}$$

where

$$P(x) = 1 + \sigma \frac{x^{\beta+1} - x}{x - 1}, \quad S(x) = 1 - x - \sigma x^{\beta+1}. \quad (46)$$

It is shown in [13] that the equation $S(x) = 0$ has $\beta+1$ roots x_j, $j = 0, 1, \ldots, \beta$, and exactly one of them, x_0 is real and positive. To prove Proposition 1 we first need to establish that these roots are distinct.

PROPOSITION 9. *The roots of $S(x) = 0$ are distinct.*

PROOF. When $S(x) = S'(x) = 0$, we have

$$1 - x - \sigma x^{\beta+1} = 0 = 1 + \sigma(\beta+1)x^{\beta}. \quad (47)$$

This implies that $x = 1 + \frac{1}{\beta} > 1$ and so that $\sigma = \frac{1-x}{x^{\beta+1}} < 0$. However, σ was assumed to be non-negative. □

Now we proceed with the proof of Proposition 1. Let $\lambda_j = 1/x_j$, then $\lambda = \lambda_j$ satisfies (6). Using that all zeros of S are distinct, we have for $Z(x,\sigma)$ the partial fraction expansion

$$Z(x,\sigma) = \sum_{j=0}^{\beta} \frac{P(x_j)}{S'(x_j)} \frac{1}{x - x_j}. \quad (48)$$

Now

$$\frac{P(x_j)}{S'(x_j)} = \frac{1 + \sigma \frac{x_j^{\beta+1} - x_j}{x_j - 1}}{-1 - (\beta+1)\sigma x_j^{\beta}} = \frac{-x_j^{-\beta}}{1 + (\beta+1)x_j^{\beta}}$$
$$= \frac{-x_j^{-\beta}}{1 + (\beta+1)\frac{1-x_j}{x_j}} = \frac{-\lambda_j^{\beta}}{(\beta+1)\lambda_j - \beta}. \quad (49)$$

Here it has been used that

$$\frac{1}{1 - x_j} = \frac{-1}{\sigma x_j^{\beta+1}}, \quad \sigma x_j^{\beta} = \frac{1 - x_j}{x_j}. \quad (50)$$

Then for $|x| < x_0$ we have

$$Z(x,\sigma) = \sum_{j=0}^{\beta} \frac{P(x_j)}{S'(x_j)} \sum_{i=0}^{\infty} \frac{-x^i}{x_j^{i+1}} \quad (51)$$
$$= \sum_{i=0}^{\infty} x^i \left(\sum_{j=0}^{\beta} \frac{\lambda_j^{\beta+1}}{(\beta+1)\lambda_j - \beta} \lambda_j^i \right), \quad (52)$$

as required.

6.2 Proof of Proposition 4

As introduced earlier,

$$\mu_0 = \lambda_0 - 1. \quad (53)$$

Then μ_0 depends on β and σ, we have $\mu_0 > 0$, and

$$\mu_0(1 + \mu_0)^{\beta} = \sigma. \quad (54)$$

By implicit differentiation with respect to β, we get from (54) that

$$\frac{\partial \mu_0}{\partial \beta} = \frac{-\mu_0(1+\mu_0)\ln(1+\mu_0)}{1 + \mu_0 + \beta\mu_0}. \quad (55)$$

In particular, both μ_0 and λ_0 decrease as a function of $\beta > 0$.

Consider the case that $0 \le \beta \le \eta - 1$. Using $\lambda_0^{\beta} = \frac{\sigma}{\lambda_0 - 1}$ we get

$$\theta(\beta,\eta,\sigma) = \sigma^2 \frac{\lambda_0^{-2\eta}}{(\lambda_0 - 1)((\beta+1)\lambda_0 - \beta)}$$
$$= \sigma^2 \frac{\lambda_0^{-2\eta}}{\mu_0(1 + \mu_0 + \beta\mu_0)}. \quad (56)$$

Now $\lambda_0^{-2\eta}$ increases as a function of β, and we shall show that $\mu_0(1+\mu_0+\beta\mu_0)$ decreases in $\beta > 0$. We have from (55) that

$$\frac{\partial}{\partial\beta}[\mu_0(1 + \mu_0 + \beta\mu_0)] = \frac{\partial}{\partial\beta}[\beta\mu_0^2 + \mu_0 + \mu_0^2]$$
$$= \mu_0^2 - \frac{1 + 2(1+\beta)\mu_0}{1 + \mu_0 + \beta\mu_0}\mu_0(1+\mu_0)\ln(1+\mu_0)$$
$$\le \mu_0(\mu_0 - (1+\mu_0)\ln(1+\mu_0)) < 0, \quad (57)$$

where the last inequality follows from $x\ln x > x - 1, x > 1$. We conclude that θ increases as a function of $\beta \in (0, \eta - 1]$.

Next we consider the case that $\beta \ge \eta + 1$. From $\lambda_0^{\beta} = \frac{\sigma}{\lambda_0 - 1}$ we get

$$\theta(\beta,\eta,\sigma) = \sigma \frac{\lambda_0^{\beta}}{(\beta+1)\lambda_0 - \beta} = \frac{\lambda_0 - 1}{(\beta+1)\lambda_0 - \beta}$$
$$= \frac{\mu_0}{1 + \mu_0 + \beta\mu_0}. \quad (58)$$

Now

$$\frac{\partial}{\partial\beta}\left(\frac{\mu_0}{1 + \mu_0 + \beta\mu_0}\right) = \frac{\frac{\partial\mu_0}{\partial\beta} - \mu_0^2}{(1 + \mu_0 + \beta\mu_0)^2} < 0, \quad (59)$$

see (55), as so θ decreases as a function of $\beta \ge \eta + 1$. Since θ depends continuously on $\beta > 0$, the result follows.

6.3 Proof of Theorem 1

The proof of the result as stated in Theorem 1 requires expanding several other results. We consider $\beta \in [\eta - 1, \eta + 1]$ so that

$$\theta(\beta,\eta,\sigma) = \sigma \frac{\lambda_0^{-\eta-1}}{(\beta+1)\lambda_0 - \beta} = \sigma \frac{(1+\mu_0)^{\eta-1}}{1 + \mu_0 + \beta\mu_0}. \quad (60)$$

From (55) it follows from a straightforward but somewhat lengthy computation that

$$\frac{\partial}{\partial\beta}[\theta(\beta,\eta,\sigma)] = \frac{-\sigma\mu_0(1+\mu_0)^{-\eta-1}}{(1 + \mu_0 + \beta\mu_0)^2} \times \left(1 - (\eta + 2 + \frac{\beta}{1 + \mu_0 + \beta\mu_0})\ln(1+\mu_0)\right). \quad (61)$$

Let

$$F(\beta,\sigma) = (\eta + 2 + \frac{\beta}{1 + \mu_0 + \beta\mu_0})\ln(1+\mu_0). \quad (62)$$

Then we have for $\beta \in [\eta - 1, \eta + 1]$ that

$$F(\beta,\sigma) > 1 \Rightarrow \theta \text{ increases strictly at } \beta, \quad (63)$$
$$F(\beta,\sigma) < 1 \Rightarrow \theta \text{ decreases strictly at } \beta. \quad (64)$$

We analyze $F(\beta,\sigma)$ in some detail, especially for values of β, σ such that $F(\beta,\sigma) = 1$. We recall here that $\mu_0 = \mu_0(\beta,\sigma)$ is a function of β and σ as well.

We fix $\beta > 0$, and we compute

$$\frac{\partial}{\partial\beta}F(\beta,\sigma) = \left[\frac{\eta+1}{\mu_0+1} + \frac{1+\beta}{1+\mu_0+\beta\mu_0} - \frac{\beta(1+\beta)\ln(1+\mu_0)}{(1+\mu_0+\beta\mu_0)^2}\right]\frac{\partial\mu_0}{\partial\eta}. \tag{65}$$

We easily get from (54) by implicit differentiation that

$$\frac{\partial\mu_0}{\partial\sigma} = \frac{\mu_0(1+\mu_0)}{\sigma(1+\mu_0+\beta\mu_0)} > 0. \tag{66}$$

Furthermore, it is easily see from (54) that $\mu_0(\beta,\sigma)\to 0$ as $\sigma\downarrow 0$ and that $\mu_0(\beta,\sigma)\to\infty$ as $\sigma\to\infty$. Hence, $\mu_0(\beta,\sigma)$ increases from 0 to ∞ as σ increases from 0 to ∞. Moreover,

$$\frac{\eta+1}{\mu_0+1} > 0, \quad 1 > \frac{\beta\ln(1+\mu_0)}{1+\mu_0+\beta\mu_0}. \tag{67}$$

It follows from (66) and (67) that $\frac{\partial}{\partial\sigma}F(\beta,\sigma) > 0$. Then, from (62) and from the fact that μ_0 increases from 0 to ∞ as σ increases from 0 to ∞, we have that $F(\beta,\sigma)$ increases from 0 to ∞ as σ increases from 0 to ∞. Therefore, for any $\beta > 0$, there is a unique $\sigma = \sigma(\beta)$ such that

$$F(\beta,\sigma) = F(\beta,\sigma(\beta)) = 1. \tag{68}$$

We shall next show that $\sigma(\beta)$ increases in $\beta\in[\eta-1,\eta+1]$. By implicit differentiation in (68), we have for $\beta\in[\eta-1,\eta+1]$

$$0 = \frac{\mathrm{d}}{\mathrm{d}\beta}[F(\beta,\sigma(\beta))] = F_\beta(\beta,\sigma(\beta)) + \sigma'(\beta)F_\sigma(\beta,\sigma(\beta)), \tag{69}$$

where F_β and F_σ denote the respective partial derivatives (and $\sigma'(\eta\pm 1)$ is the left and right derivative for $+$ and $-$, respectively). We already know that $F_\sigma > 0$, and we shall show now that $F_\beta(\beta,\sigma(\beta)) < 0$. To that end, we compute, using (55) that

$$\begin{aligned}&\frac{\partial}{\partial\beta}[F(\beta,\sigma)]\\ &= -\ln(1+\mu_0)\Big[(\eta+2+\frac{\beta}{1+\mu_0+\beta\mu_0})\frac{\mu_0}{1+\mu_0+\beta\mu_0}\\ &\quad -\frac{1+\mu_0-\beta(1+\beta)\mu_0'}{(1+\mu_0+\beta\mu_0)^2}\Big].\end{aligned} \tag{70}$$

Next, from (62) and (68) we have that

$$\mu_0 \ge \ln(1+\mu_0) = \frac{1}{\eta+2+\frac{\beta}{1+\mu_0+\beta\mu_0}}, \tag{71}$$

and so

$$\begin{aligned}&\frac{\partial F}{\partial\beta}(\beta,\sigma(\beta))\\ &\le -\ln(1+\mu_0)\left[\frac{1}{1+\mu_0+\beta\mu_0} - \frac{1+\mu_0-\beta(1+\beta)\mu_0'}{(1+\mu_0+\beta\mu_0)^2}\right]_{\sigma=\sigma(\beta)}\\ &= \frac{-\beta\ln(1+\mu_0)}{(1+\mu_0+\beta\mu_0)^2}\left[\mu_0+(1+\beta)\mu_0'\right]_{\sigma=\sigma(\beta)}\\ &= \frac{-\mu_0\beta\ln(1+\mu_0)}{(1+\mu_0+\beta\mu_0)^2}\left[1-(1+\beta)\frac{(1+\mu_0)\ln(1+\mu_0)}{1+\mu_0+\beta\mu_0}\right]_{\sigma=\sigma(\beta)},\end{aligned} \tag{72}$$

where (55) has been used once more. Finally, from (68),

$$\begin{aligned}&(1+\beta)\frac{(1+\mu_0)\ln(1+\mu_0)}{1+\mu_0+\beta\mu_0}\Big|_{\sigma=\sigma(\beta)}\\ &= \frac{(1+\beta)(1+\mu_0)}{(\eta+2)(1+\mu_0+\beta\mu_0)+\beta}\Big|_{\sigma=\sigma(\beta)} < 1\end{aligned} \tag{73}$$

since $0<\beta\le\eta+1$ and $\mu_0>0$. Hence, $F_\beta(\beta,\sigma(\beta)) < 0$ as required. It now follows from (69) and from $F_\sigma(\beta,\sigma(\beta)) > 0$ that $\sigma'(\beta) > 0$ when $\beta\in[\eta-1,\eta+1]$.

We have now shown that $\sigma(\beta)$ increases in $\beta\in[\eta-1,\eta+1]$. Next we let

$$\sigma_{\min} := \sigma(\eta-1) < \sigma(\eta+1) =: \sigma_{\max}. \tag{74}$$

For $\sigma\in[\sigma_{\min},\sigma_{\max}]$ there is defined the inverse function $\beta(\sigma)\in[\eta-1,\eta+1]$ that increases in σ. It follows then from

$$F(\beta(\sigma),\sigma) = 1, \quad F_\beta(\beta(\sigma),\sigma) < 0 \tag{75}$$

and (61)-(64) that $\theta(\beta,\eta,\sigma)$ is maximal at $\beta=\beta(\sigma)$ when $\sigma\in[\sigma_{\min},\sigma_{\max}]$.

We shall now complete the proof of Theorem 1. Let $\beta\in[\sigma_{\min},\sigma_{\max}]$, and assume that $\sigma\le\sigma_{\min}$. Then $\sigma<\sigma(\beta)$ and so $F(\beta,\sigma) < F(\beta,\sigma(\beta)) = 1$ since F increases in σ. Hence, θ strictly decreases at β. Similarly, θ strictly increases at $\beta\in(\eta-1,\eta+1)$ when $\sigma\ge\sigma_{\max}$. It follows that θ strictly decreases in $\beta\in[\eta-1,\eta+1]$ when $\sigma\le\sigma_{\min}$ and that θ strictly increases in $\beta\in[\eta-1,\eta+1]$ when $\sigma\ge\sigma_{\max}$. Finally, when $\sigma\in(\sigma_{\min},\sigma_{\max})$, we have that

$$\begin{aligned}&F(\eta-1,\sigma) > F(\eta-1,\sigma_{\min})\\ &\quad = 1 = F(\eta+1,\sigma_{\max}) > F(\eta+1,\sigma),\end{aligned} \tag{76}$$

showing that θ strictly increases at $\beta=\eta-1$ and strictly decreases at $\beta=\eta+1$, and assumes its maximum at $\beta=\beta(\sigma)$.

6.4 Proof of Theorem 2

We shall show below that

$$(\eta+2+\frac{\eta-1}{1+\eta\kappa})\ln(1+\kappa) < 1 < (\eta+2+\frac{\eta+1}{1+(\eta+2)\kappa})\ln(1+\kappa) \tag{77}$$

when $\kappa=\tau/(\eta+1)$. Assuming this, we recall that (for fixed $\beta>0$) μ_0 strictly increases in σ and vice versa. When now

$$\sigma_- = \kappa(1+\kappa)^{\eta-1}, \tag{78}$$

we have that $F(\eta-1,\sigma_-) < 1$ and so $\sigma_- < \sigma_{\min}$ since F is increasing in σ. Similarly, when

$$\sigma_+ = \kappa(1+\kappa)^{\eta+1}, \tag{79}$$

we have from (77) that $F(\eta+1,\sigma_+) > 1$, and so $\sigma_+ > \sigma_{\max}$. Therefore,

$$\begin{aligned}\sigma_{\max}-\sigma_{\min} &< \sigma_+-\sigma_- = \kappa(1+\kappa)^{\eta+1}((1+\kappa)^2-1)\\ &= 2\left(1+\frac{\tau}{\eta+1}\right)^{\eta-1}\left(\frac{\tau}{\eta+1}\right)\left(1+\frac{\tau}{\eta+1}\right)\\ &\le 2\mathrm{e}^\tau\left(\frac{\tau}{\eta+1}\right)^2(1+\frac{\tau}{\eta+1}).\end{aligned} \tag{80}$$

It remains to show (77). As to the first inequality in (77) we have

$$1-(\eta+2+\frac{\eta-1}{1+\eta\kappa})\ln(1+\kappa)>1-(\eta+2+\frac{\eta-1}{1+\eta\kappa})\kappa$$
$$=\frac{1}{1+\eta\kappa}(1-(\eta+1)\kappa-\eta(\eta+2)\kappa^2)$$
$$>\frac{1}{1+\eta\kappa}(1-(\eta+1)\kappa-((\eta+1)\kappa)^2)=0 \quad (81)$$

when $\kappa=\tau/(\eta+1)$ since $1-\tau-\tau^2=0$. As to the second inequality of (77) we have

$$1-(\eta+2+\frac{\eta+1}{1+(\eta+2)\kappa})\ln(1+\kappa)$$
$$<1-(\eta+2+\frac{\eta+1}{1+(\eta+2)\kappa})(\kappa-\frac{1}{2}\kappa^2)$$
$$=\frac{1}{1+(\eta+2)\kappa}\Big(1-(\eta+1)\kappa-((\eta+1)\kappa)^2-$$
$$\kappa^2(\eta+3/2-\frac{1}{2}(\eta+2)^2\kappa)\Big). \quad (82)$$

With $\kappa=\tau/(\eta+1)$ we have

$$1-(\eta+1)\kappa-((\eta+1)\kappa)^2=0 \quad (83)$$

as before, and

$$\eta+\frac{3}{2}-\frac{1}{2}(\eta+2)^2\kappa=\eta+\frac{3}{2}-\frac{(\eta+2)^2}{2(\eta+1)}\tau>0,\quad \eta\geq 0 \quad (84)$$

since $\tau=\frac{1}{2}(\sqrt{5}-1)<\frac{3}{4}$ (which is the minimum value of $2(\eta+3/2)(\eta+1)(\eta+2)^{-2},\eta\geq 0$). This shows the second inequality in (77).

6.5 Proof of Proposition 5

To prove Proposition 5 we need the following result:

PROPOSITION 10. *With $\beta=\eta+\gamma$ where $-1\leq\gamma\leq 1$, we have*

$$\sigma(\beta)=\mu(1+\mu)^{\eta+\gamma}, \quad (85)$$

where

$$\mu=\frac{\tau}{\eta+\alpha+\mathcal{O}(\eta^{-1})},\qquad \alpha=\frac{(5+2\gamma)\tau+1}{2(2\tau+1)}, \quad (86)$$

and the $\mathcal{O}$ holds uniformly in $\gamma\in[-1,1]$.

PROOF. We have $\sigma(\beta)=\mu(1+\mu)^{\beta}$ where μ is the unique solution of the equation

$$(\eta+2+\frac{\beta}{1+(1+\beta)\mu})\ln(1+\mu)=1. \quad (87)$$

We know from the proof of Theorem 2 that $\mu=\mathcal{O}(\eta^{-1})$. Multiplying (87) by $1+(1+\beta)\mu$ and developing

$$\ln(1+\mu)=\mu-\frac{1}{2}\mu^2+\mathcal{O}(\mu^3), \quad (88)$$

we get

$$(\eta\beta+\frac{1}{2}\eta+\frac{3}{2}\beta+1)\mu^2+(\eta+1)\mu-1=\frac{1}{2}(\eta+2)(\beta+1)\mu^3+\mathcal{O}(\eta^{-2}). \quad (89)$$

Next let $\alpha\in\mathbb{R}$ be independent of η and use $\beta=\eta+\gamma$ to write

$$\eta\beta+\frac{1}{2}\eta+\frac{3}{2}\beta+1=(\eta+\alpha)^2+(2+\gamma-2\alpha)\eta+\frac{3}{2}\gamma+1-\alpha^2. \quad (90)$$

Together with $\eta+1=\eta+\alpha+1-\alpha$, we obtain

$$(\eta+\alpha)^2\mu^2+(\eta+\alpha)\mu-1$$
$$=\frac{1}{2}(\eta+2)(\eta+\gamma+1)\mu^3-((2+\gamma-2\alpha)\eta+\frac{3}{2}\gamma+1-\alpha^2)\mu^2$$
$$-(1-\alpha)\mu+\mathcal{O}(\eta^{-2}). \quad (91)$$

We now take α such that the whole second member of (91) is $\mathcal{O}(\eta^{-2})$. Using that $\mu=\frac{\tau}{\eta}+\mathcal{O}(\eta^{-2})$, this leads to

$$\frac{1}{2}\tau^3-(2+\gamma-2\alpha)\tau^2-(1-\alpha)\tau=0, \quad (92)$$

and this yields the α in (86). The polynomial $x^2+x-1=0$ has a zero of first order at $x=\tau$. Hence with α as in (86) we see from $(\eta+\alpha)^2\mu^2+(\eta+\alpha)\mu-1=\mathcal{O}(\eta^{-2})$ that $(\eta+\alpha)\mu=\tau+\mathcal{O}(\eta^{-2})$. This gives the result. □

Now we proceed to prove Proposition 5. We use the result of Proposition 10. Thus

$$\sigma(\eta+\gamma)=\mu(1+\mu)^{\eta+\gamma}, \quad (93)$$
$$\mu=\frac{\tau}{\eta+\alpha+\mathcal{O}(\eta^{-1})}=\frac{\tau}{\eta+\alpha}(1+\mathcal{O}(\eta^{-2})). \quad (94)$$

By elementary considerations

$$\sigma(\eta+\gamma)$$
$$=\frac{\tau}{\eta+\alpha}(1+\frac{\tau}{\eta+\alpha})^{\eta+\gamma}(1+\mathcal{O}(\eta^{-2}))$$
$$=\frac{\tau}{\eta+\alpha}\exp[(\eta+\gamma)(\frac{\tau}{\eta+\alpha}-\frac{\tau^2}{2(\eta+\alpha)})](1+\mathcal{O}(\eta^{-2}))$$
$$=\frac{\tau e^{\tau}}{\eta+\alpha}(1+\frac{(\gamma-\alpha)\tau-\frac{1}{2}\tau^2}{\eta})(1+\mathcal{O}(\eta^{-2})). \quad (95)$$

Then letting $\gamma=\pm 1$ and

$$\alpha(1)=\frac{7\tau+1}{2(2\tau+1)},\quad \alpha(-1)=\frac{3\tau+1}{2(2\tau+1)} \quad (96)$$

in accordance with Proposition 10, it follows that

$$\sigma(\eta+1)-\sigma(\eta-1)=\frac{\tau e^{\tau}}{\eta^2}\Big(\alpha(-1)-\alpha(1)+(1-\alpha(1))\tau$$
$$+(1+\alpha(-1))\tau\Big)+\mathcal{O}(\eta^{-3})$$
$$=\frac{\tau e^{\tau}}{\eta^2}\frac{2\tau^2}{2\tau+1}+\mathcal{O}(\eta^{-3}). \quad (97)$$

Finally, it follows easily from $\tau^2+\tau=1$ that $\tau^3(7+4\tau)=2\tau+1$.

6.6 Proof of Proposition 6

Since $\sigma>0$ is fixed, it follows from (see the proof of Theorem 2)

$$\sigma_{\max}<\sigma_+=\frac{\tau}{\eta+1}\left(1+\frac{\tau}{\eta+1}\right)^{\eta+1}<\frac{\tau e^{\tau}}{\eta+1} \quad (98)$$

that $\sigma_{\max} < \sigma$ when η is large enough. By Theorem 1

$$\max\theta = \theta(\eta+1) = \frac{\lambda_0 - 1}{(\eta+2)\lambda_0 - \eta - 1} = \frac{\mu_0}{(\eta+2)\mu_0 + 1} = \frac{1}{\eta+2}\frac{1}{1+\frac{1}{(\eta+2)\mu_0}}, \quad (99)$$

where μ_0 is the unique positive real μ root of $\mu(1+\mu)^{\eta+1} = \sigma$. We shall show that

$$(\eta+2)\mu_0 \geq \ln\sigma, \quad (100)$$
$$(\eta+2)\mu_0 = \ln(\eta+1) + \mathcal{O}(\ln\ln(\eta+1)), \quad \eta\to\infty, \quad (101)$$

uniformly in $\sigma \in [\epsilon, M]$, where $\epsilon > 0$ and $M > \epsilon$ are fixed. To show (100), we note from $\mu_0(1+\mu_0)^{\eta+1} = \sigma$ that

$$(\eta+1)\mu_0 \geq (\eta+1)\ln(1+\mu_0) = \ln\sigma - \ln\mu_0. \quad (102)$$

Next $\sigma = \mu_0(1+\mu_0)^{\eta+1} \geq \mu_0^{\eta+2}$, and so $\ln\mu_0 \leq \frac{1}{\eta+2}\ln\sigma$. Therefore

$$(\eta+1)\mu_0 \geq \ln\sigma - \frac{1}{\eta+2}\ln\sigma = \frac{\eta+1}{\eta+2}\ln\sigma, \quad (103)$$

and (100) follows. As to (101), we first observe from (55) that μ_0 decreases in η when $\sigma > 0$ is fixed. Hence $L = \lim_{\eta\to\infty}\mu_0$ exists, and it follows from $\mu_0(1+\mu_0)^{\eta+1} = \sigma$ that $L = 0$. Thus, μ_0 decreases to 0 as $\eta\to\infty$. Then, from (102) we get that $(\eta+1)\mu_0$ increases to ∞ as $\eta\to\infty$. All this holds uniformly in $\sigma\in[\epsilon,M]$: since μ_0 increases in σ, the right-hand side of (102) is bounded below by $\ln\epsilon - \ln\mu_0(\sigma = M)$. Now take $\eta_0 > 0$ such that $(\eta+1)\mu_0 \geq \sigma$ when $\eta\geq\eta_0$ and $\epsilon\leq\sigma\leq M$. Then from $\mu_0(1+\mu_0)^{\eta+1} = \sigma$ we have

$$(\eta+1)\ln(1+\mu_0) = \ln\sigma - \ln\mu_0 \leq \ln(\eta+1)\mu_0 - \ln\mu_0 \leq \ln(\eta+1) \quad (104)$$

when $\eta\geq\eta_0$ and $\epsilon\leq\sigma\leq M$. Hence, when $\eta\geq\eta_0$,

$$\mu_0 \leq \exp\left[\frac{\ln(\eta+1)}{\eta+1}\right] - 1 = \frac{\ln(\eta+1)}{\eta+1} + \mathcal{O}\left(\left(\frac{\ln(\eta+1)}{\eta+1}\right)^2\right), \quad (105)$$

where the $\mathcal{O}$ holds uniformly in $\sigma\in[\epsilon,M]$. Then, by (102),

$$\begin{aligned}(\eta+1)\mu_0 &\geq \ln\sigma - \ln\left(\exp\left[\frac{\ln(\eta+1)}{\eta+1}\right] - 1\right)\\ &= \ln\sigma - \ln(\frac{\ln(\eta+1)}{\eta+1}\left(1 + \mathcal{O}\left(\frac{\ln(\eta+1)}{\eta+1}\right)\right)\\ &= \ln(\eta+1) - \ln\ln(\eta+1) + \ln\sigma + \mathcal{O}\left(\frac{\ln(\eta+1)}{\eta+1}\right),\end{aligned} \quad (106)$$

with $\mathcal{O}$ holding uniformly in $\sigma\in[\epsilon,M]$ and $\eta\geq\eta_0$. From (105) and (106) we get (100) uniformly in $\sigma\in[\epsilon,M]$.

7. REFERENCES

[1] N. Abramson. The ALOHA system - another alternative for computer communications. In *Proc. of AFIPS*, pages 281–285, 1970.

[2] S. Asmussen. *Applied Probability and Queues.* Springer-Verlag, New York, second edition, 2003.

[3] Y. Baryshnikov, E. G. Coffman, Jr., and P. Jelenković. Space filling and depletion. *Journal of Applied Probability*, 41(3):691–702, 2004.

[4] R. Boorstyn and A. Kershenbaum. Throughput analysis of multihop packet radio. In *Proc. of ICC*, pages 1361–1366, 1980.

[5] C. Bordenave, D. McDonald, and A. Proutière. Performance of random medium access control, an asymptotic approach. In *Proc. of ACM Sigmetrics*, pages 1–12, 2008.

[6] N. G. de Bruijn. *Asymptotic methods in analysis.* Dover Publications Inc., New York, third edition, 1981.

[7] D. Denteneer, S. Borst, P. Van de Ven, and G. Hiertz. IEEE 802.11s and the philosophers' problem. *Statistica Neerlandica*, 62(3):283–298, 2008.

[8] M. Durvy, O. Dousse, and P. Thiran. Modeling the 802.11 protocol under different capture and sensing capabilities. In *Proc. of INFOCOM*, pages 2356–2360, 2007.

[9] M. Durvy, O. Dousse, and P. Thiran. Self-organization properties of CSMA/CA systems and their consequences on fairness. *IEEE Transactions on Information Theory*, 55(3), 2009.

[10] L. Kleinrock and F. Tobagi. Packet switching in radio channels: part I - carrier sense multiple-access modes and their throughput-delay characteristics. *IEEE Transactions on Communications*, 23(12):1400–1416, 1975.

[11] T. Lin and J. Hou. Interplay of spatial reuse and SINR-determined data rates in CSMA/CA-based, multi-hop, multi-rate wireless networks. In *Proc. of INFOCOM*, pages 803–811, 2007.

[12] H. Ma, R. Vijaykumar, S. Roy, and J. Zhu. Optimizing 802.11 wireless mesh networks based on physical carrier sensing. IEEE/ACM Transactions on Networking, 2009 (to appear).

[13] E. Pinsky and Y. Yemini. The asymptotic analysis of some packet radio networks. *IEEE Journal on Selected Areas in Communications*, 4(6):938–945, 1986.

[14] S. Rajagopalan, J. Shin, and D. Shah. Network adiabetic theorem: An efficient randomized protocol for contention resolution. In *Proc. of ACM Sigmetrics/Performance*, pages 133–144, 2009.

[15] F. Tobagi and L. Kleinrock. Packet switching in radio channels: part II - the hidden terminal problem in carrier sense multiple-access and the busy-tone solution. *IEEE Transactions on Communications*, 23(12):1417–1433, 1975.

[16] P. van de Ven, J. van Leeuwaarden, T. Denteneer, and A. Janssen. Spatial fairness in wireless multi-access networks. In *Proc. of ValueTools*, 2009.

[17] X. Wang and K. Kar. Throughput modelling and fairness issues in CSMA/CA based ad-hoc networks. In *Proc. of INFOCOM*, pages 23–34, 2005.

[18] X. Yang and N. Vaidya. On the physical carrier sense in wireless ad hoc networks. In *Proc. of INFOCOM*, pages 2525–2535, 2005.

[19] M. Zafer and E. Modiano. Blocking probability and channel assignment in wireless networks. *IEEE Transactions on Wireless Communications*, 5(4):869–879, 2006.

[20] H. Zhai and Y. Fang. Physical carrier sensing and spatial reuse in multirate and multihop wireless ad hoc networks. In *Proc. of INFOCOM*, pages 1–12, 2006.